

Electronic Supplementary Information

Highly Efficient Photoluminescent Cu(I)-PyrPHOS-metallopolymers

Daniel Volz,^{a,c} Astrid Hirschbiel,^b Daniel M. Zink,^c Jana Friedrichs,^c Martin Nieger,^d Thomas Baumann,^c Stefan Bräse*^a and Christopher Barner-Kowollik*^b

^a*Institute of Organic Chemistry, Karlsruhe Institute of Technology (KIT), Fritz-Haber-Weg 6, 76131 Karlsruhe, Germany and Institute of Toxicology and Genetics, Karlsruhe Institute of Technology (KIT), Hermann-von-Helmholtz-Platz 1, 76344 Eggenstein-Leopoldshafen, Germany. E-mail: braese@kit.edu*

^b*Preparative Macromolecular Chemistry, Institute of Chemical Technology and Polymer Chemistry, Karlsruhe Institute of Technology (KIT), Engesserstr. 18, 76131 Karlsruhe, Germany, and Institute for Biological Interfaces, Karlsruhe Institute of Technology (KIT), Hermann-von-Helmholtz Platz 1, 76344 Eggenstein-Leopoldshafen, Germany. E-mail: christopher.barner-kowollik@kit.edu*

^c*cynora GmbH, Hermann-von-Helmholtz-Platz 1, 76344 Eggenstein-Leopoldshafen, Germany. E-mail: info@cynora.com*

^d*Laboratory of Inorganic Chemistry, University of Helsinki, P.O. Box 55, FI-00014, Finland.*

Experimental section.

General. Reactions were carried out at ambient temperature (r.t.) unless noted otherwise and the following abbreviations were used: calc. (theoretical value), found (measured value). Information is given in mass percent. Routine monitoring of reactions was performed using Silica gel coated aluminium plates (Merck, silica gel 60, F254), which were analyzed under UV-light at 254 nm and / or dipped in a solution of molybdate phosphate (5% phosphor molybdic acid in ethanol) and potassium permanganate (0.45 g potassium permanganate and 2.35 g of sodium carbonate in 90 ml of water) and heated with a heat gun. CuI (99.999% trace metals basis) was purchased by Sigma Aldrich and used without further purification. MePyrPHOS was synthesized according to a recently published procedure.² To preclude any effects due to trace impurities, the ligand was distilled twice (0.3 mbar, 220 °C) prior to use. All solvents were purchased by Aldrich and VWR and were at least of 99.5% purity. AIBN (Sigma Aldrich) was recrystallized in methanol and stored at -18 °. Vinylbenzyl chloride (Sigma Aldrich) was destabilized by passing over a column of basic alumina prior to use and stored at -18°C. For flash chromatography and extractions, solvents of p.a. (per analysis) quality were employed. The solvents were purchased commercially (Roth) and utilized without purification. The following absolute solvents were used for synthesis (Roth, < 50 ppm H₂O): dichloromethane, tetrahydrofurane, diethylether, toluene, dioxane, dimethylformamide. Reactions with air and / or moisture-sensitive reagents were performed according to the usual Schlenk techniques under a nitrogen atmosphere. Therefore, the glassware, equipped with a PTFE-coated magnetic bar, was repeatedly heated under high vacuum with a heat gun and flushed with nitrogen. Subsequently, the glassware was equipped with rubber septa in a nitrogen counterflow. Demineralized water was used. Small batches were carried out in a heated reaction block (H+P Labortechnik GmbH, controlled by Tele Variomag module) with an integrated magnetic stirrer. Headspace vials with volumes of 5 and 10 mL, sealed with a teflon-coated rubber septum and aluminium cap, were employed as reaction vessels. Nitrogen, which was used as inert gas, was injected through a cannula. If necessary, the reactions were cooled by a cryostat.

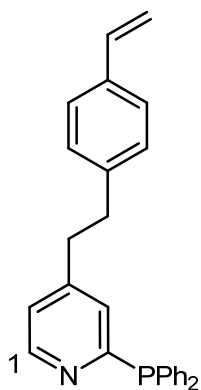
Analytical techniques. Proton Nuclear Magnetic Resonance (¹H NMR) spectra were recorded on a Bruker AM 400 (400 MHz) spectrometer as solutions in CDCl₃. Chemical

shifts are expressed in parts per million (ppm) downfield from tetramethylsilane (TMS) and are referenced to CHCl_3 (7.26 ppm) as internal standard. All coupling constants are absolute values and J values are expressed in hertz (Hz). The description of signals include: s = singlet, bs = broad singlet, d = doublet, t = triplet, m = multiplet. The spectra were analyzed according to first order. The signal abbreviations include: Ar-H = aromatic proton; Carbon Nuclear Magnetic Resonance (^{13}C NMR) spectra were recorded on a Bruker AM 400 (100 MHz) spectrometer as solutions in CDCl_3 . The signals were allocated through DEPT-technology (DEPT = Distortionless Enhancement by Polarization Transfer). The signal abbreviations include: C-Ar = aromatic carbon, CH_3/CH = primary or tertiary carbon atom, CH_2 = secondary carbon atom, C_{quart} = quaternary carbon atom. Electron impact mass spectrometry (MS (EI)) and high resolution mass spectrometry (HRMS) were recorded on a Finnigan MAT 90 (70 eV). The molecular fragments are quoted as the relation between mass and charge (m/z), the intensities as a percentaged value relative to the intensity of the base signal (100%). The abbreviation $[\text{M}^+]$ refers to the molecular ion. Fast atom bombardment (FAB) spectra were measured in 3-Nitrobenzylalcohol as matrix. The spectra of the complexes showed cluster ions of copper iodide and the ligands, having the general formula $[\text{Cu}_n\text{I}_{n-1}(\text{ligand})_m]^+$. The abbreviation N,P and PR_3 refer to the ligands in this context. Infrared spectroscopy (IR) was conducted on a FT-IR Bruker IFS 88. IR spectra of solids were recorded in KBr, and as thin films on KBr for oils and liquids. The deposit of the absorption band was given in wave numbers in cm^{-1} . The forms and intensities of the bands were characterized as follows: s = strong 10–40% T, m = medium 40–70% T, w = weak 70–90% T, vw = very weak 90–100% T, br = broad. Elemental analysis (EA) was measured on an instrument by Elementar vario MICRO. The values for carbon (C), hydrogen (H) and nitrogen (N) are defined in mass percent. Gel permeation chromatography (GPC) was performed on a Polymer Laboratories (Varian) PL-GPC 50 Plus Integrated System, comprising an autosampler, a PLgel 5 μm bead-size guard column (50 \times 7.5 mm), one PLgel 5 μm Mixed E column (300 \times 7.5 mm) three PLgel 5 μm Mixed C columns (300 \times 7.5 mm) and a differential refractive index detector using THF as the eluent at 35 $^\circ\text{C}$ with a flow rate of 1 mL min^{-1} . Additionally, N,N -dimethylacetamide (DMAc) containing 0.3 wt % LiBr was employed as eluent at 50 $^\circ\text{C}$ with a flow rate of 1.0 mL min^{-1} . The SEC system was calibrated using linear poly(styrene) standards ranging from 160 to 6×10^6 $\text{g} \cdot \text{mol}^{-1}$ and linear poly(methyl methacrylate) standards

ranging from 700 to 2×10^6 g·mol⁻¹. All GPC calculations were carried out relative to poly(styrene) calibration (Mark Houwink parameters $K = 14.1 \times 10^{-5}$ dL·g⁻¹; $\alpha = 0.7$).¹

Synthesis and spectroscopic properties of the new compounds.

Part 1: Model complexes and monomers



2-Diphenylphosphino-4-(4-vinylphenethyl)-pyridine (m0).

Diphenylphosphino-4-methylpyridine (MePyrPHOS, 3.50 g, 12.6 mmol, 1.00 eq.) was dissolved in 100 mL of dry THF and cooled to $-78\text{ }^{\circ}\text{C}$ under nitrogen atmosphere. Lithiumdiisopropylamide (freshly prepared by mixing dry diisopropylamine (2.0 mL, 13.9 mmol, 1.10 eq.) in 10 mL THF with buthyl lithium (5.6 mL, 13.9 mmol, 1.10 eq., 2.2 M in cyclohexane) at $0\text{ }^{\circ}\text{C}$) was added dropwise. The reaction mixture was stirred for 10 h and was allowed to warm to $-5\text{ }^{\circ}\text{C}$. The resulting reddish solution was cooled to $-78\text{ }^{\circ}\text{C}$ again and 4-vinylbenzylchloride (2 mL, 13.9 mmol, 1.10 eq.) in 10 mL THF was added dropwise. The reaction mixture was stirred at ambient temperature overnight. The mixture was quenched with 4 mL of water, the solvent was evaporated and the product was purified by column chromatography (cyclohexane / ethyl acetate = 5 / 1) to yield the title compound as a colorless oil. Yield: 3.90 g (79%, 9.9 mmol). ^1H NMR (300 MHz, CDCl_3): δ = 8.51 (d, 1H, $^3J_{\text{HH}} = 5.1\text{ Hz}$, C=N-CH), 7.29 – 7.18 (m, 16H, Ar-H), 6.61 (dd, 1H, $^3J_{\text{HH}} = 18.6\text{ Hz}$, 11.7 Hz, Ar-CH=CH₂), 5.62 (dd, 1H, $^3J_{\text{HH}} = 18.6\text{ Hz}$, CH_{cis}H_{trans}), 5.14 (dd, 1H, $^3J_{\text{HH}} = 11.7\text{ Hz}$, CH_{cis}H_{trans}), 2.73 (m, 4H, CH₂CH₂) ppm. ^{13}C NMR (100 MHz, CDCl_3): δ = 164.03 (C_{quart}), 151.04 (C_{quart}), 150.34 (CH), 136.57 (CH), 136.25 (C_{quart}), 135.79 (C_{quart}), 134.29 (CH), 132.20 (C_{quart}), 131.93 (CH), 129.02 (CH), 128.68 (CH), 128.57 (CH), 128.36 (CH), 126.31 (CH), 125.47 (CH), 122.61 (CH), 113.35 (=CH₂), 37.14 (-CH₂-), 36.09 (-CH₂-) -5.05 ppm . ^{31}P NMR (101 MHz, CDCl_3): δ = -5.05 ppm . – IR (ATR): ν = 3440 (w), 3051 (s), 3017 (m), 2925 (m), 2858 (w), 1903 (w), 1816 (w), 1702 (w), 1629 (vs), 1587 (m), 1547 (m), 1511 (m), 1479 (m), 1454 (s), 1435 (vs), 1407 (m), 1387 (m), 1308 (vw), 1279 (vw), 1195 (s), 1120 (m), 1093 (w), 1069 (vw), 1027 (w), 990 (m), 907 (m), 842 (s), 744 (vs), 723 (s), 696 (vs), 618 (vw), 547 (s), 504 (m), 462 (w), 429 (vw) cm^{-1} . – MS (70 eV, EI), m/z (%): 393 (37) [M]⁺, 294.2 (2) [M-C₆H₄-CH=CH₂]⁺, 277.2 (100) [M-CH₂-C₆H₄-CH=CH₂]⁺, 262.2 (8) [M-C₂H₄-C₆H₄-CH=CH₂]⁺, 199 (50), 107 (18), 77 (13). – HR-EIMS (C₂₇H₂₄NP): calc. 393.1646; found. 393.1653.

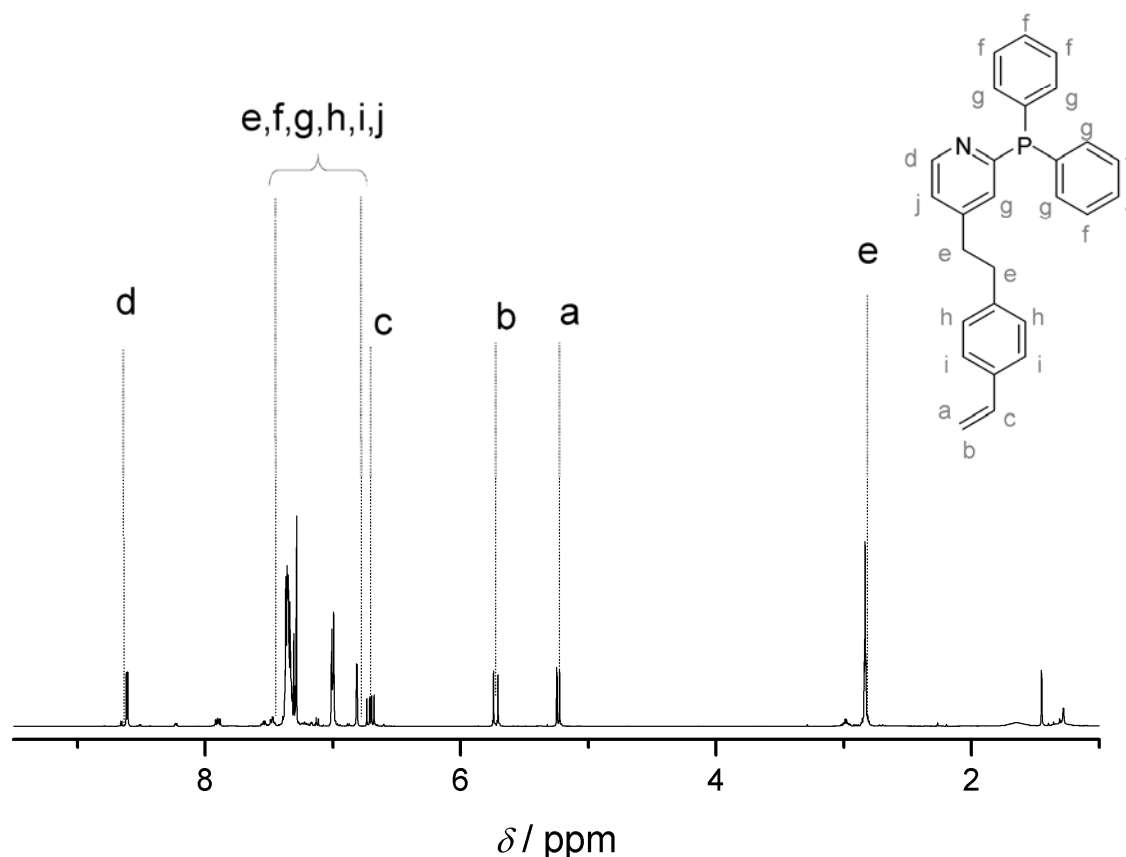


Figure S1: ¹H NMR (300 MHz, CDCl₃, 25 °C) spectrum of monomer **m0**. For assignment of the peaks refer to the structure within the figure.

(2-Diphenylphosphino-4-(4-vinyl-phenethyl)-pyridine)(triphenylphosphine)₂Cu₂I₂ (**m1**). The title compound was synthesized according to the general procedure and obtained as a light green powder (88%, 730 mg, 0.56 mmol). ¹H-NMR (400 MHz, CDCl₃): δ = 8.50 – 8.15 (bs, 1 H), 7.60 – 7.40 (m, Ar-H, 14 H) 7.30 – 6.70 (m, Ar-H, 33 H), 6.61 (dd, 1H, ³J_{HH} = 18.4 Hz, 11.3 Hz, Ar-CH=CH₂), 5.62 (dd, 1H, ³J_{HH} = 18.4 Hz, CH_{cis}H_{trans}), 5.14 (dd, 1H, ³J_{HH} = 11.3 Hz, CH_{cis}H_{trans}), 2.73 (m, 4H, CH₂CH₂) ppm. ³¹P NMR (101 MHz, CDCl₃): δ = -5.05 (PyPHOS), -15.25 (PPh₃) ppm. IR (ATR): ν = 3051 (m), 2971 (m), 2349 (vw), 1962 (vw), 1897 (vw), 1811 (vw), 1626 (vw), 1594 (w), 1544 (vw), 1511 (vw), 1478 (m), 1433 (s), 1386 (vw), 1362 (vw), 1309 (vw), 1264 (vw), 1233 (vw), 1198 (vw), 1157 (vw), 1092 (m), 1074 (m), 1028 (w), 995 (w), 909 (w), 843 (w), 742 (vs), 692 (vs), 619 (w), 513 (vs), 473 (m), 426 (w) cm⁻¹. MS (FAB-MS): 325 [CuPR₃]⁺, 456 [CuN,P]⁺, 515 [Cu₂I(PR₃)]⁺, 587 [Cu(PR₃)₂]⁺, 648 [Cu₂I(N,P)]⁺, 718 [Cu(N,P)(PR₃)]⁺, 777 [Cu₂I(PR₃)₂]⁺, 838 [Cu₃I₂(PR₃)]⁺, 908

$[\text{Cu}_2\text{I}(\text{N,P})(\text{PR}_3)]^+$, 1039 $[\text{Cu}_2\text{I}(\text{N,P})_2]^+$, 1100 $[\text{Cu}_3\text{I}_2(\text{N,P})(\text{PR}_3)]^+$, 1231 $[\text{Cu}_3\text{I}_2(\text{N,P})_3]^+$. EA: calc. for $\text{C}_{63}\text{H}_{54}\text{NP}_3\text{Cu}_2\text{I}_2 \times \text{MTBE}$: C 58.88, H 4.80, N 1.01; found: C 58.66, H 4.70, N 0.67.

(2-Diphenylphosphino-4-methyl-pyridine)(triphenylphosphine)₂Cu₂I₂ (**m2**): This compound has been synthesized according to the literature.⁴

(2-Diphenylphosphino-4-(4-vinyl-phenethyl)-pyridine)₃Cu₂I₂ (**m3**) The title compound was synthesized according to the general procedure and obtained as a light yellow powder (70%, 546 mg, 0.35 mmol). ¹H NMR (300 MHz, CDCl₃): δ = 8.71 (bs, 3H, C=N-CH), 7.50 – 7.00 (m, 48H, Ar-H), 6.60 (dd, 3H, ³J_{HH} = 18.2 Hz, 11.3 Hz, Ar-CH=CH₂), 5.68 (dd, 3H, ³J_{HH} = 18.2 Hz, CH_{cis}H_{trans}), 5.21 (dd, 3H, ³J_{HH} = 11.3 Hz, CH_{cis}H_{trans}), 2.80 – 2.60 (m, 12H, CH₂CH₂) ppm. ³¹P NMR (101 MHz, CDCl₃): δ = -10.10 (PyrPHOS) ppm. IR (ATR): ν = 3051 (w), 1627 (vw), 1586 (m), 1544 (w), 1510 (w), 1479 (w), 1433 (m), 1386 (w), 1181 (vw), 1092 (m), 1027 (vw), 988 (m), 903 (m), 841 (s), 702 (vs), 692 (vs), 499 (vs), 467 (s), 436 (s) cm⁻¹. MS (FAB-MS): 456 $[\text{CuN,P}]^+$, 648 $[\text{Cu}_2\text{I}(\text{N,P})]^+$, 837 $[\text{Cu}_3\text{I}_2(\text{N,P})]^+$, 848 $[\text{Cu}(\text{N,P})_2]^+$, 1039 $[\text{Cu}_2\text{I}(\text{N,P})_2]^+$. EA: calc. for $\text{C}_{81}\text{H}_{72}\text{N}_3\text{P}_3\text{Cu}_2\text{I}_2$: C 62.31, H 4.65, N 2.69; found: C 61.98, H 4.78, N 2.55.

(2-Diphenylphosphino-4-methyl-pyridine)₃Cu₂I₂ (**m4**): This compound has been synthesized according to the literature.³

Part 2: Polymerizations

Table S1: Reaction conditions and concentrations for the polymerization of monomer **m0**

polymer	solvent	initiator	CTA	c_{Initiator}	c_{Monomer}	time
p0	1,4-dioxane	VAZO88	DBTTC	1272 mmol L ⁻¹	2.52 mmol L ⁻¹	20 h
p4	toluene	AIBN	DBTTC	1.67 mmol L ⁻¹	38.5 mmol L ⁻¹	24 h
p5	toluene	AIBN	CPDB	1.52 mmol L ⁻¹	38.5 mmol L ⁻¹	24 h
p6	toluene	AIBN	-	7.70 mmol L ⁻¹	38.5 mmol L ⁻¹	24 h

Table S2: Stock solutions for loading of PyrPHOS-polymers

solution	ligand	solvent	Product
s1	PPh ₃	acetonitrile	p1
s2	P(<i>p</i> -OMe-C ₆ H ₅) ₃	acetonitrile	p2
s3	P(C ₈ H ₁₇) ₃	acetonitrile/toluene 1:1	p3

Poly-(2-(diphenylphosphino)-4-(4-vinylphenyl) pyridine) (**p0**). The title compound was synthesized according to the general procedure with 1,4-dioxane as the solvent, DBTTC as chain transfer agent and 1,1'-azobis(cyanocyclohexane) (VAZO-88) as the initiator. SEC results (DMAc): $M_n = 25\ 000\ \text{g}\cdot\text{mol}^{-1}$, $D = 1.52$.

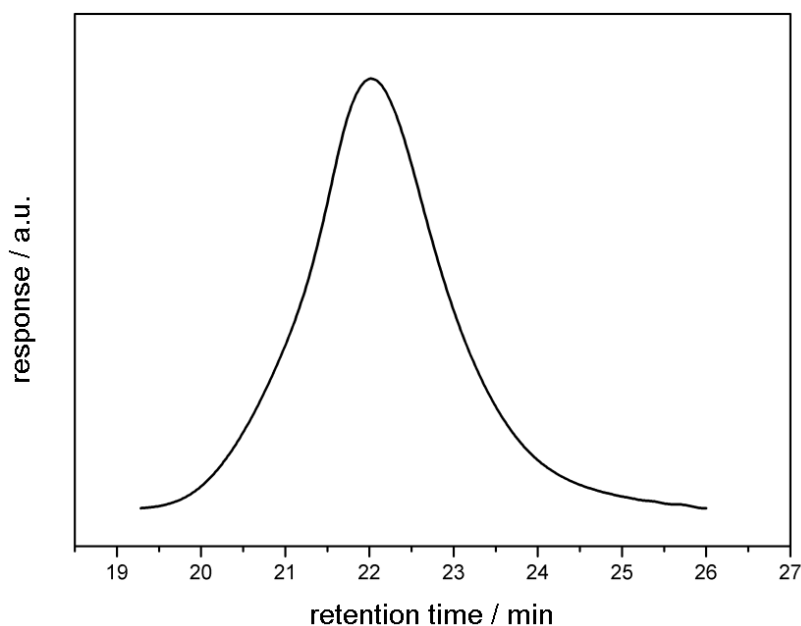


Figure S2: SEC elugram of polymer **p0** in DMAc. The SEC system was calibrated using linear polystyrene standards in DMAc 35 °C. **p0**: $M_n = 25\ \text{kDa}$ and $D = 1.55$.

The SEC data suggests that the polymerization process was reasonably well controlled. The number average molecular weight, M_n , determined *via* SEC measurement with a value of $25\ 000\ \text{g}\cdot\text{mol}^{-1}$ equals to 50% conversion with a pre-calculated molecular weight of $40\ 000\ \text{g}\cdot\text{mol}^{-1}$, assuming total conversion. 50% conversion after a reaction time of 20 h correlates with the 36% conversion after 10 h reaction time. Since the SEC is calibrated with polystyrene standards and therefore does not provide true values for polymer **p0**, a deviation from the theoretical value is expected.

Characterization of the bulk-metallopolymers (p1-p3). As noted in the main text, the metallopolymers could not be analyzed by SEC, since the samples were not sufficiently soluble in common solvents employed for this technique (THF, DMAc, toluene). Additionally, no $^1\text{H-NMR}$ spectra could be measured, due to solubility issues.

Poly-(2-(diphenylphosphino)-4-(4-vinylphenyl)pyridine)(PPh₃)₂Cu₂I₂ (p1). The employed reaction conditions are collated in Table S2. Due to low solubility, no satisfactory NMR spectra could be obtained. IR (ATR): $\nu = 3046$ (w), 2913 (w), 1600 (broad, w), 1585 (m), 1543 (w), 1509 (m), 1478 (m), 1432 (s), 1385 (m), 1182 (w), 1156 (w), 1092 (m), 1026 (w), 997 (w), 837 (w), 739 (vs), 689 (vs), 495 (vs) cm^{-1} . EA (end groups were not taken into account, calculated with quantitative loading): calc. C 58.25, H 4.19; N 1.08; found C 58.90, H 4.52, N 1.44, S 0.52.

Poly-(2-(diphenylphosphino)-4-(4-vinylphenyl)pyridine)(P(p-MeO-C₆H₅)₂Cu₂I₂ (p2). The employed reaction conditions are collated in Table S2. Due to low solubility, no satisfactory NMR spectra could be obtained. IR (ATR): $\nu = 3048$ (w), 2923 (w), 1600 (broad, w), 1589 (m), 1545 (w), 1498 (m), 1480 (m), 1434 (s), 1387 (m), 1286 (w), 1249 (m), 1178 (m), 1096 (m), 1027 (w), 826 (w), 798 (m), 742 (vs), 693 (vs), 617 (vw), 501 (vs) 471 (s) cm^{-1} . EA (end groups were not taken into account, calculated with quantitative loading): calc. C 56.03, H 4.50; N 0.95; found C 56.90, H 4.53, N 1.28, S 0.49.

Poly-(2-(diphenylphosphino)-4-(4-vinylphenyl)pyridine)(P(n-oct)₃)₂Cu₂I₂ (p3). The employed reaction conditions are collated in Table S2. Due to low solubility, no satisfactory NMR spectra could be obtained. IR (ATR): $\nu = 3048$ (w), 2923 (m), 2853 (w), 1604 (broad, vw), 1587 (m), 1545 (w), 1509 (w), 1480 (m), 1434 (s), 1387 (m), 1184 (w), 1094 (m), 1027 (w), 988 (w), 836 (w), 742 (s), 692 (vs), 546 (vw), 501 (vs) 471 (s) cm^{-1} . EA (end groups were not taken into account, calculated with quantitative loading): calc. C 59.43, H 8.38; N 0.92; found C 57.03, H 7.84, N 1.38, S 0.46.

Poly-(2-(diphenylphosphino)-4-(4-vinylphenyl)pyridine)(PPh₃)₂Cu₂I₂ (p4). The employed reaction conditions are collated in Table S1. Due to low solubility, no satisfactory NMR

spectra could be obtained. IR: see above. EA (end groups were not taken into account): calc. C 58.25, H 4.19; N 1.08; found C 59.17, H 4.35, N 1.28, S 0.68.

Poly-(2-(diphenylphosphino)-4-(4-vinylphenyl)pyridin)(PPh₃)₂Cu₂I₂ (p5). The employed reaction conditions are collated in Table S1. Due to low solubility, no satisfactory NMR spectra could be obtained. IR: see above. EA (end groups were not taken into account): calc. C 58.25, H 4.19; N 1.08; found C 57.88, H 4.20, N 1.57, S 0.80.

Poly-(2-(diphenylphosphino)-4-(4-vinylphenyl)pyridin)(PPh₃)₂Cu₂I₂ (p6). The employed reaction conditions are collated in Table S1. Due to low solubility, no satisfactory NMR spectra could be obtained. IR: see above. EA (end groups were not taken into account): calc. C 58.25, H 4.19; N 1.08; found C 58.58, H 4.20, N 1.57.

Poly-(2-(diphenylphosphino)-4-(4-vinylphenyl)pyridin)(PPh₃)₂Cu₂I₂ (p7). The employed reaction conditions are collated in Table S1. Due to low solubility, no satisfactory NMR spectra could be obtained. IR (ATR): $\nu = 3046$ (w), 2913 (w), 1600 (broad, w), 1585 (m), 1543 (w), 1509 (m), 1478 (m), 1432 (s), 1385 (m), 1182 (w), 1156 (w), 1092 (m), 1026 (w), 997 (w), 837 (w), 739 (vs), 689 (vs), 495 (vs) cm^{-1} . EA (Per repeating unit: C₆₃H₅₄Cu₂I₂NP₃, 1297.02): calc. C 58.25, H 4.19; N 1.08; found C 58.33, H 4.11, N 1.03.

Figure S4 shows the IR spectra of the products **p4–p6** as well as the spectra of the monomer **m1** for comparison (430 to 3800 cm^{-1}). The signal at 1627 cm^{-1} may be assigned to the C=C-stretching vibration and is only present in the spectrum of the monomeric complexes **m1** and **m3**. However, the relative intensity is not high and other, more prominent bands (as a result of the Cu(I)-PyrPHOS-unit) in close proximity, hinder its quantitative evaluation. We thus chose the vinyl-CH₂ out-of-plane bending mode (906 cm^{-1}) and the CH_{vinyl} out-of-plane bending mode (841 cm^{-1}), which were present in the finger-print region, as an indicator for completeness of the polymerization. Figure S4 shows that these two peaks are only present in the IR spectrum of the monomeric complex **m1**.

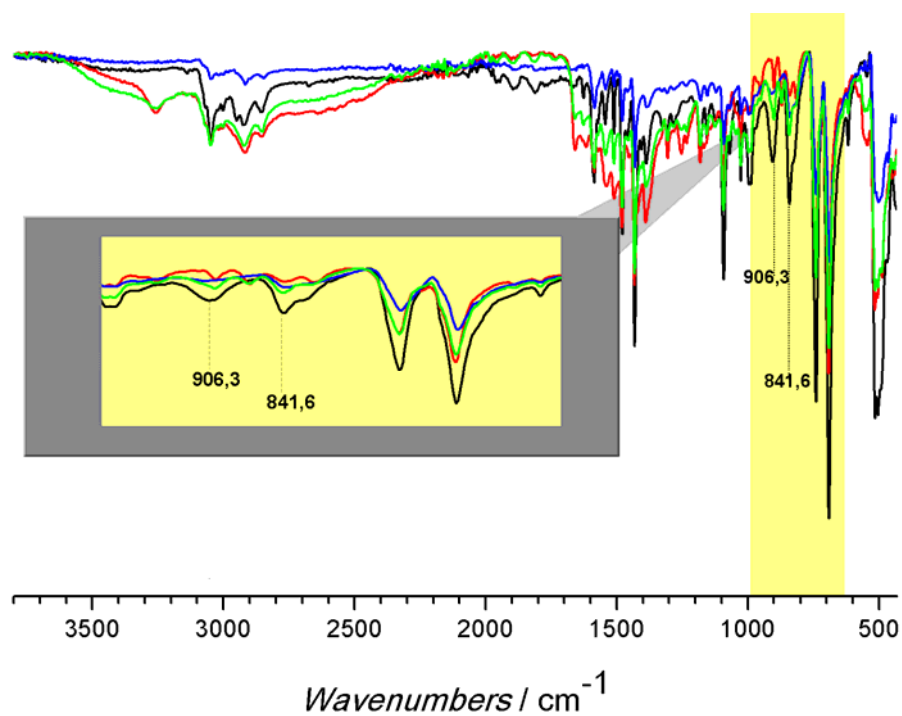


Figure S3. IR spectra of monomeric complex **m1** (black curve) and the metallopolymers **p4** – **p6** (green, blue and red, respectively) in direct comparison. The vinyl-CH₂ out-of-plane bending mode (906 cm^{-1}) and the CH_{vinyl} out-of-plane bending mode (841 cm^{-1}) are only present in the monomer and thus confirm the absence of quenching styrene-moieties.

Quenching in p4 and p5: UV/VIS Spectra of DBTTC and CPDB in dichloromethane.

UV/Vis-Absorption spectra were measured on a Thermo Scientific (Evolution 201) UV-visible spectrophotometer in dichloromethane at concentrations of 10^{-4} to 10^{-5} M.

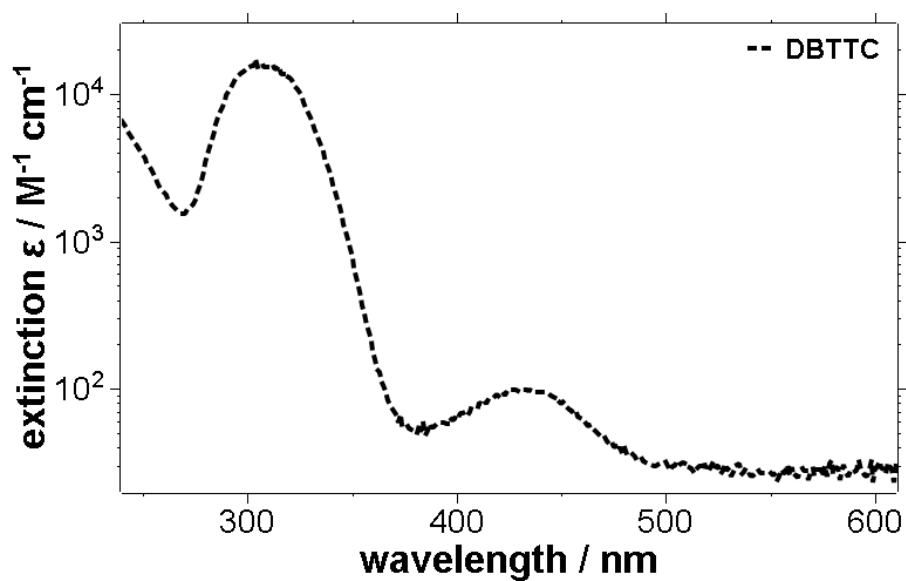


Figure S4: Absorption spectrum of DBTTC in dichloromethane. DBTTC absorbs in the region of the excitation maximum (350 nm).

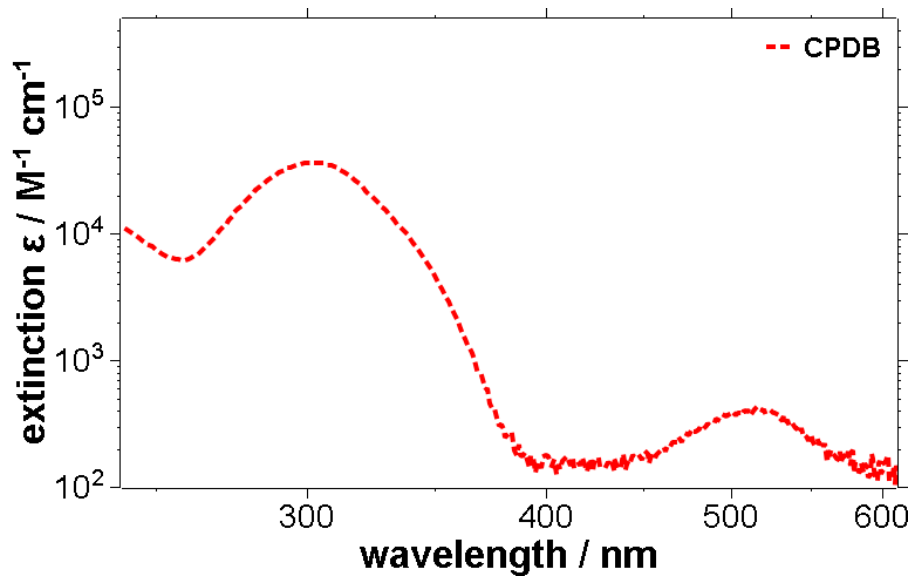


Figure S5: Absorption spectrum of CPDB in dichloromethane. CPDB absorbs in the region of the excitation maximum (350 nm) as well as in the region of the emission of the Cu(I)-PyrPHOS-complexes around 540 nm.

Thermoanalytical experiments

Thermogravimetric analyses (TGA) were measured with a TGA/SDTA 851e instrument (Mettler Toledo) in an Al₂O₃ pan with a constant heating rate of 5 °C/min to a maximum temperature of 500 °C. Both the sample gas and the balance gas were nitrogen (80 mL min⁻¹). Sample amounts of approximately 5 mg were used. The DSC scan (Figure S6) of **m1** clearly shows an exothermic reaction starting around 135 °C, which was assigned to a thermally initiated polymerization. Judging from the shape of the band, expulsion of 1 equivalent of methyl-*tert*-butyl ether (MTBE), which has also been shown with X-Ray-diffraction and elemental analysis, occurs in the same region. No further reactions could be detected below 230 °C, the upper limit for this experiment. This is in good agreement with similar styrene-substituted complexes.^{6,7} The processing temperature was thus set to 170°C.

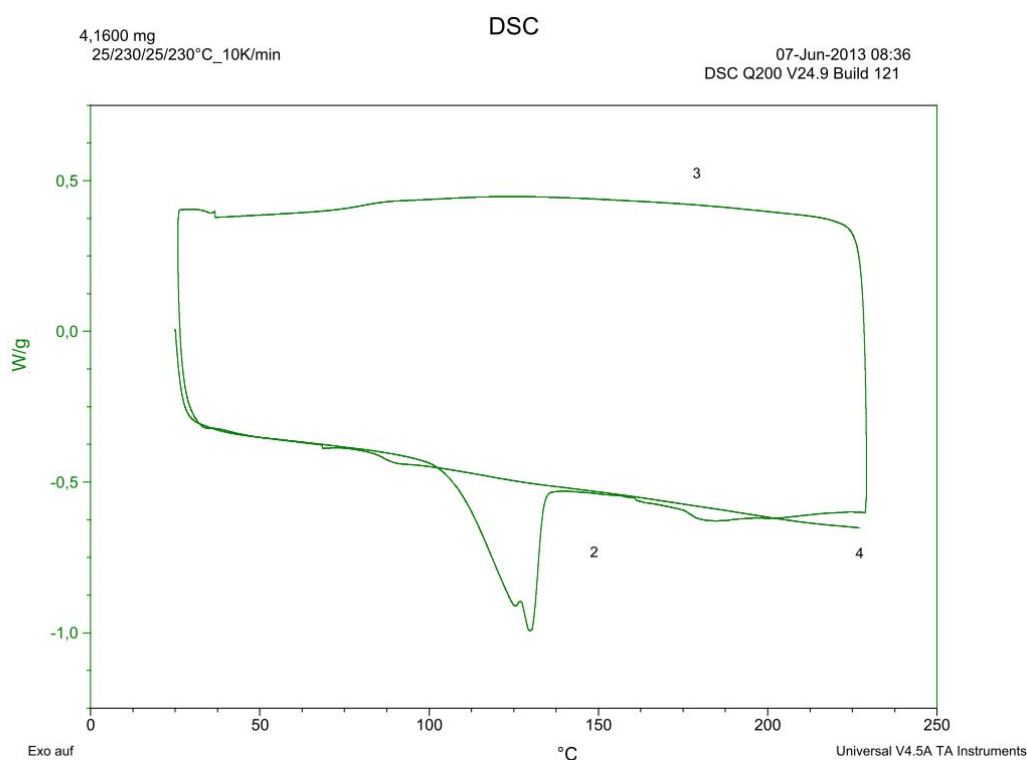
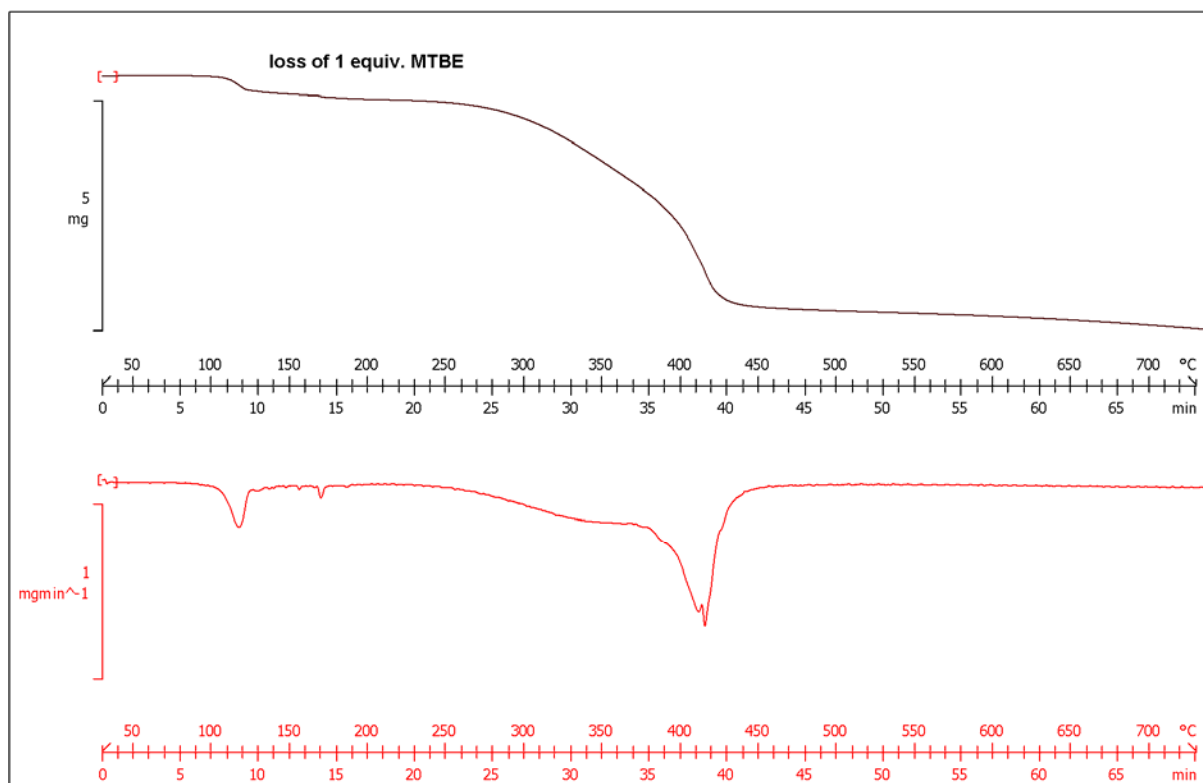


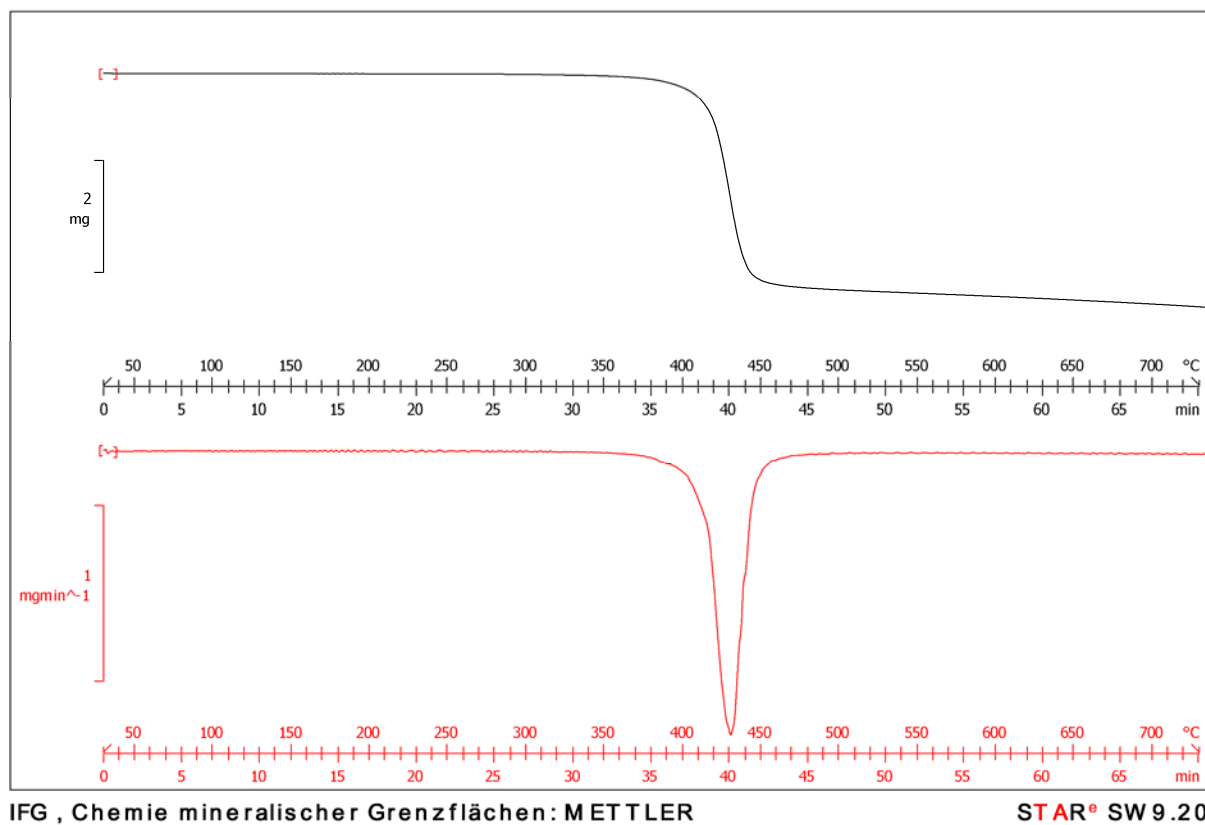
Figure S6: DSC trace for compound **m1**. In the first heating scan, an exothermic reaction is visible around 130 °C.



IFG , Chemie mineralischer Grenzflächen: METTLER

STAR® SW 9.20

Figure S7: TGA trace of compounds **m1**. Around 110 °C, intercalated methyl-*tert*-butyl ether is released. Thermal decomposition of this compound starts around 260 °C.



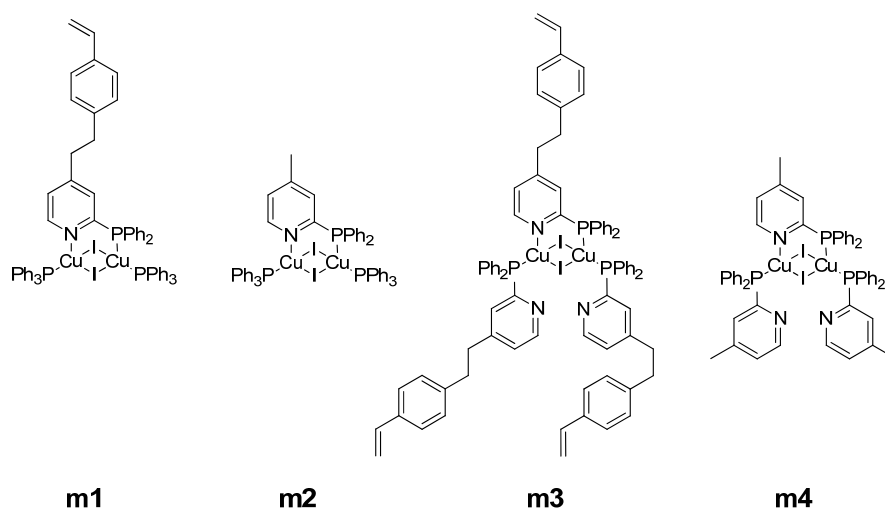
IFG , Chemie mineralischer Grenzflächen: METTLER STAR® SW 9.20
Figure S8: TGA trace for compound **p7**. Thermal decomposition of this compound starts around 430 °C.

PL characterization of m1 and m3

Photophysical measurements. Absorption spectra were measured on a Thermo Scientific (Evolution 201) UV-visible spectrophotometer in acetonitrile. Emission and excitation spectra in the solid state were measured with a Horiba Scientific FluoroMax-4 spectrofluorometer using a JX monochromator and a R928P PMT detector. Fluorescence lifetime measurements were recorded and detected on the same system using the time-correlated single photon-counting (TCSPC) method with the FM-2013 accessory and a TDSPC hub from Horiba Yvon Jobin. For this, a NanoLED 370 was used as excitation source ($\lambda = 370$ nm, 1.5 ns pulse). Decay curves were analyzed with the software DAS-6 and DataStation provide by Horiba Yvon Jobin. The quality of the fit was determined by the Chi-Square-method by Pearson.⁶ The quality factor χ^2 should be as close to unity as possible. The definition for the factor is described in Equation S2 with e_i being the value proposed by the fit and o_i being the actual value

$$\chi^2 = \sum_{k=1}^i \frac{(e_i - o_i)^2}{e_i} \quad \text{Equation S1}$$

For the determination of PLQY ϕ , an absolute PL quantum yield measurement system from Hamamatsu Photonics was used. The system consisted of a photonic multichannel analyzer PMA-12, a model C99200-02G calibrated integrating sphere and a monochromatic light source L9799-02 (150 W Xe- and Hg-Xe-lamps). Data analysis was carried out with the PLQY measurement software U6039-05, provided by Hamamatsu Photonics.



Scheme S1: Molecular structures of the model compounds studied herein.

Full spectra for compounds **m2** and **m4** have already been published.³⁻⁵

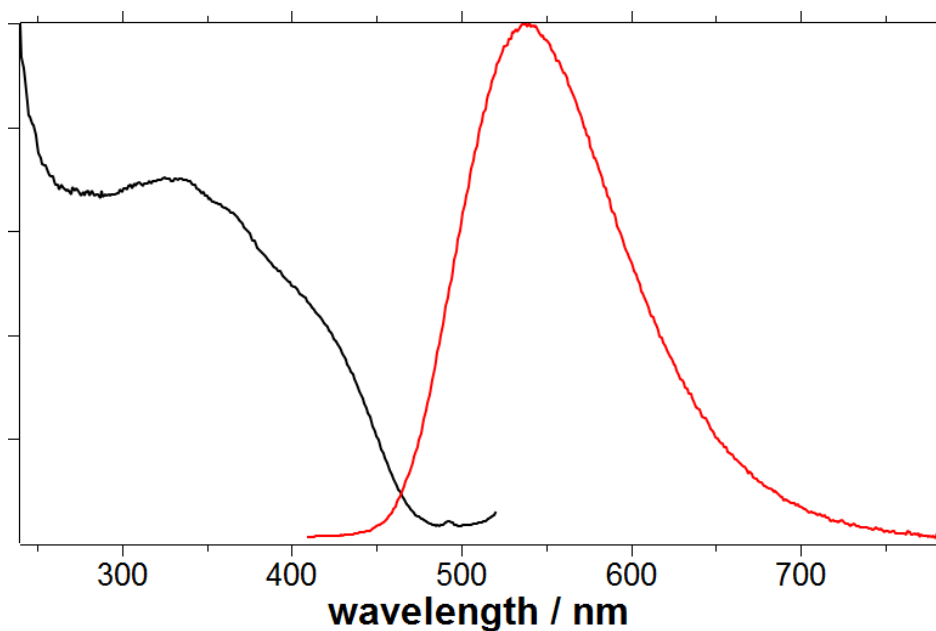


Figure S9: PL spectra of compound **m1** (powder spectra) at ambient temperature. Black: excitation spectrum ($\lambda_{em} = 550$ nm), red: emission spectrum ($\lambda_{exc} = 350$ nm).

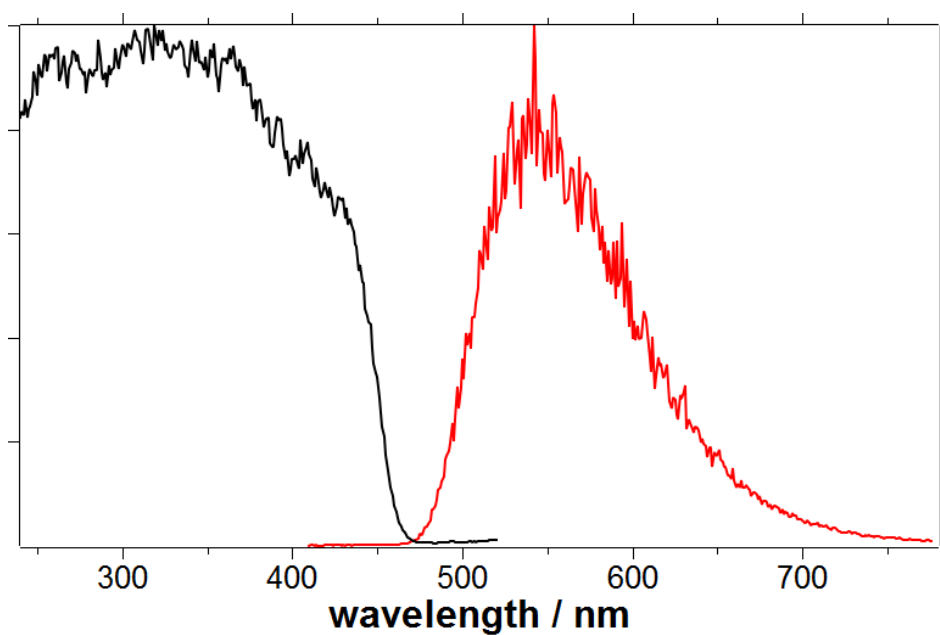


Figure S10: PL spectra of compound **m1** (powder spectra) at 77 K. Black: excitation spectrum ($\lambda_{em} = 550$ nm), red: emission spectrum ($\lambda_{exc} = 350$ nm)

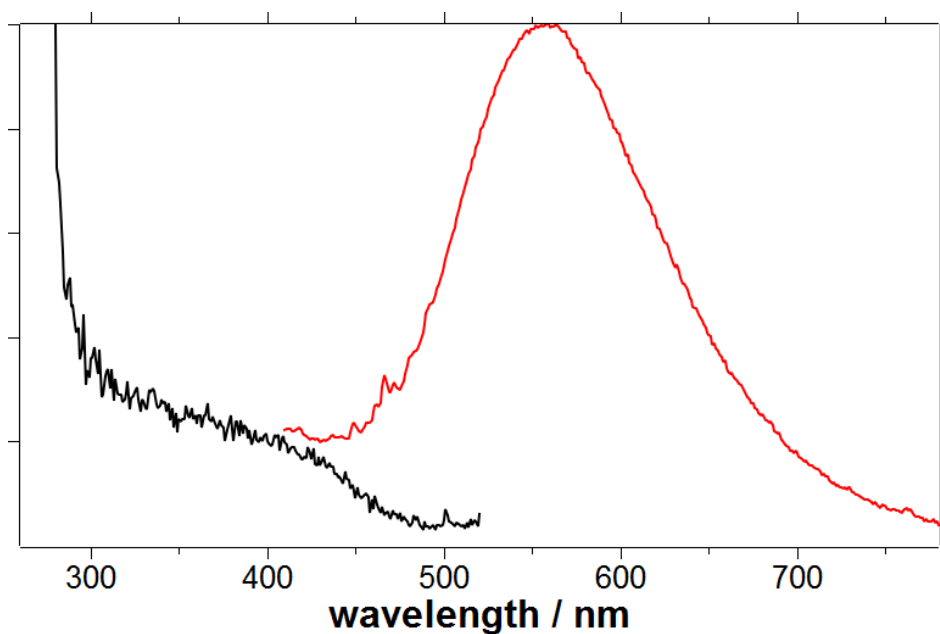


Figure S11: PL spectra of compound **m3** (powder spectra) at room temperature. Black: excitation spectrum ($\lambda_{em} = 550$ nm), red: emission spectrum ($\lambda_{exc} = 350$ nm)

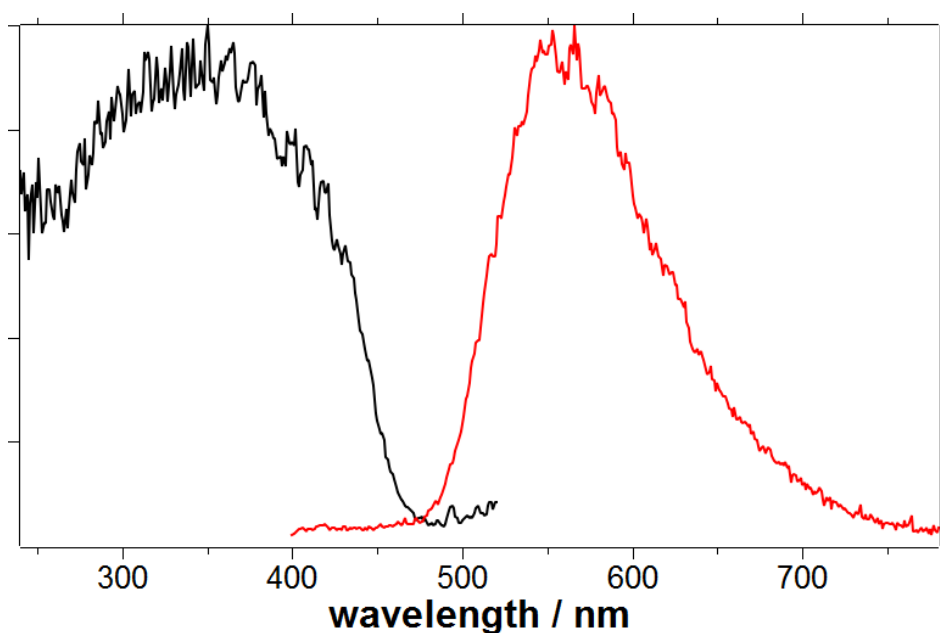


Figure S12: PL spectra of compound **m3** (powder spectra) at 77 K. Black: excitation spectrum ($\lambda_{\text{em}} = 550$ nm), red: emission spectrum ($\lambda_{\text{exc}} = 350$ nm)

Table S3: Overview: PLQY ϕ and emission decay time τ at r.t. and 77 K (powder)

comp.	r.t.					77 K				
	λ [nm]	ϕ	τ [μs]	k_r	k_{nr} [10^6 s^{-1}]	λ [nm]	ϕ	τ [μs]	k_r	k_{nr} [10^6 s^{-1}]
m1	537	0.04	1.57	0.03	1.54	546	0.47	18.2	0.03	0.02
m3	555	0.04	1.71	0.02	0.56	561	0.22	23.9	0.01	0.03

Table S4: Time-correlated single photon counting (TCSPC). Fitted decay data and τ at r.t. and 77 K (powder)

compound	r.t.					77 K			
	A_1	$\tau(1)$ [μs]	A_2	$\tau(2)$ [μs]	χ^2	$\langle\tau\rangle$ [μs]	χ^2	$\langle\tau\rangle$ [μs]	
m1	0.77	0.20	0.23	1.57	1.15	0.52	1.15	18.2	
m3	0.73	0.24	0.27	1.71	1.18	0.63	1.19	23.9	

The normalized decay kinetics $I(t)$ was fitted using equation S3.

$$I(t) = A_1 \exp(-t/\tau(1)) + A_2 \exp(-t/\tau(2)) \quad \text{Equation S2}$$

At 77 K, a monoexponential function gave sufficiently good fitting results (equation S4).

$$I(t) = A_1 \exp(-t/\tau(1)) \quad \text{Equation S3}$$

The quality of the fit is expressed according to Pearson in χ^2 , which should be as close to unity as possible.⁸

X-ray structure of **m1**

X-ray diffraction study of m1. The single-crystal X-ray diffraction studies were carried out on a Bruker Apex Duo diffractometer at 120 K using Mo $K\alpha$ radiation ($\lambda = 0.71073$ Å). Direct Methods (SHELXS-97) (G. M. Sheldrick, *Acta Crystallogr.* 2008, **A64**, 112-122) were used for structure solution and full-matrix least-squares refinement on F^2 (SHELXL-97) (G. M. Sheldrick, *Acta Crystallogr.* 2008, **A64**, 112-122). H atoms were refined using a riding model. A semi-empirical absorption correction was applied.

Crystal data of **m1**

$C_{63}H_{54}Cu_2I_2NP_3 \cdot C_5H_{12}O$

$M_r = 1387.01$

Triclinic, $P-1$ (no.2)

$a = 11.0591$ (5) Å

$b = 11.7309$ (5) Å

$c = 24.4524$ (11) Å

$\alpha = 85.982$ (1)°

$\beta = 77.364$ (2)°

$\gamma = 80.162$ (1)°

$V = 3048.2$ (2) Å³

$Z = 2$

$F(000) = 1396$

$D_x = 1.511$ Mg m⁻³

Mo $K\alpha$ radiation, $\lambda = 0.71073$ Å

Cell parameters from 8031 reflections

$\theta = 1-26^\circ$

$\mu = 1.83$ mm⁻¹

$T = 120$ K

Blocks, pale yellow

$0.16 \times 0.12 \times 0.08$ mm

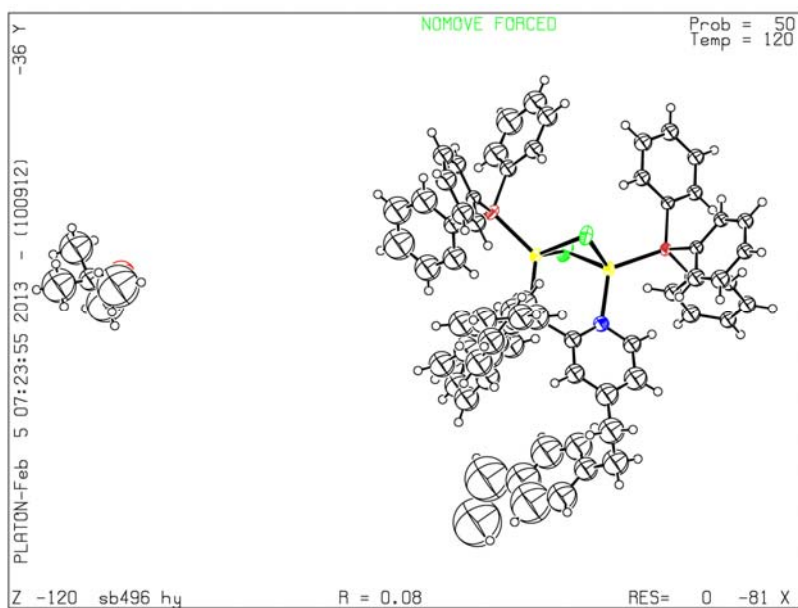


Figure S13: Structure of **m1** (displacement parameters are drawn at 50% probability level, only I, Cu and P atoms refined anisotropically, plot created by the checkCIF/PLATON report).

Data collection of **m1**

Bruker Apex Duo diffractometer	11796 independent reflections
Radiation source: fine-focus sealed tube	9218 reflections with $I > 2\sigma(I)$
Graphite monochromator	$R_{\text{int}} = 0.022$
rotation in phi and ω , 0.5 deg. scans	$\theta_{\text{max}} = 26.0^\circ$, $\theta_{\text{min}} = 1.9^\circ$
Absorption correction: multi-scan <i>SADABS</i>	$h = -13 \rightarrow 13$
$T_{\text{min}} = 0.814$, $T_{\text{max}} = 0.888$	$k = -14 \rightarrow 14$
20677 measured reflections	$l = -27 \rightarrow 30$

Refinement of **m1**

Refinement on F^2

Least-squares matrix: full

$$R[F^2 > 2\sigma(F^2)] = 0.084$$

$$wR(F^2) = 0.265$$

$$S = 1.02$$

11796 reflections

256 parameters

99 restraints

Primary atom site location: structure-invariant direct methods

Secondary atom site location: difference Fourier map

Hydrogen site location: inferred from neighbouring sites

H-atom parameters constrained

$$w = 1/[\sigma^2(F_o^2) + (0.150P)^2 + 36.P]$$

$$\text{where } P = (F_o^2 + 2F_c^2)/3$$

$$(\Delta/\sigma)_{\max} = 0.001$$

$$\Delta_{\max} = 2.41 \text{ e } \text{\AA}^{-3}$$

$$\Delta_{\min} = -1.53 \text{ e } \text{\AA}^{-3}$$

DFT-calculations of m1

DFT calculations. DFT calculations were performed using the BP86^{9,10} functional with the resolution-of-identity approximation⁹⁻¹² and the def2-SV(P)^{14,15} basis set. For numerical integration, the m4 grid was employed. The initial structure was obtained from single-crystal X-ray diffraction data. All calculations were carried out using the Turbomole program package (version 6.4).¹⁶ Analytic vibrational frequency analysis has been performed to ensure that the stationary points in the ground state and in the lowest triplet state (which was calculated using an unrestricted formalism) are true minima. The lowest TDDFT singlet excitation can be assigned to a HOMO-LUMO excitation both at the optimized ground state geometry and at the optimized triplet geometry. Since the HOMO is located mainly on the Cu₂I₂-core and the LUMO is located on the N[^]P ligand, this corresponds to an (MX)LCT charge transfer transition.

Table S5: Comparison between selected bond distances for the S₀- and T₁ state and X ray data (Å)

	Cu-Cu	Cu ₁ -I ₁	Cu ₁ -I ₂	Cu ₂ -I ₁	Cu ₂ -I ₂	Cu ₁ -N	Cu ₂ -P ₁	Cu ₁ -P ₂	Cu ₂ -P ₃
S ₀	2.66	2.70	2.73	2.72	2.72	2.11	2.30	2.29	2.31
T ₁	2.52	2.685	2.75	2.72	2.69	2.03	2.32	2.33	2.32
X-ray	2.7568	2.68	2.66	2.67	2.68	2.09	2.25	2.25	2.26

Table S6: Comparison between selected bond angles for S₀- and T₁ state and X ray data (degree)

	Cu-I ₁ -Cu	Cu-I ₂ -Cu	I-Cu-Cu-I
S ₀	58.85	58.44	148.39
T ₁	55.62	55.11	123.36
X-ray	62.04	62.28	144.02

References

1. H. L. Wagner, *J. Phys. Chem. Ref. Data*, 1985, **14**, 1101.
2. D. Volz, T. Baumann, H. Flügge, M. Mydlak, T. Grab, M. Bächle, C. Barner-Kowollik, and S. Bräse, *J. Mater. Chem.*, 2012, **22**, 20786.
3. D. Volz, M. Nieger, J. Friedrichs, T. Baumann, and S. Bräse, *Langmuir*, 2013, **29**, 3034–3044.
4. D. M. Zink, M. Bächle, T. Baumann, M. Nieger, M. Kühn, C. Wang, W. Klopfer, U. Monkowius, T. Hofbeck, H. Yersin, and S. Bräse, *Inorg. Chem.*, 2013, **52**, 2292–305.
5. D. Volz, D. M. Zink, T. Bocksrocker, J. Friedrichs, M. Nieger, T. Baumann, S. Bräse, and U. Lemmer, *Chem. Mater.*, 2013, doi 10.1021/cm4010807.
6. E. Otsuki, H. Sato, A. Kawakami, H. Taka, H. Kita, and H. Usui, *Thin Solid Films*, 2009, **518**, 703–706.
7. B. Ma, F. Lauterwasser, L. Deng, C. S. Zonte, B. J. Kim, J. M. J. Fréchet, C. Borek, and M. E. Thompson, *Chem. Mater.*, 2007, **19**, 4827–4832.
8. K. Pearson, *Philos. Mag.*, 1900, **50**, 157–175.
9. A. D. Becke, *Phys. Rev. A*, 1988, **38**, 3098–3100.
10. J. Perdew, *Phys. Rev. B*, 1986, **33**, 8822–8824.
11. M. Häser and R. Ahlrichs, *J. Comput. Chem.*, 1989, **10**, 104–111.
12. F. Weigend and M. Häser, *Theo. Chim. Acta*, 1997, **97**, 331–340.
13. M. Sierka, A. Hogekamp, and R. Ahlrichs, *J. Chem. Phys.*, 2003, **118**, 9136.
14. F. Weigend and R. Ahlrichs, *Phys. Chem. Chem. Phys.*, 2005, **7**, 3297–305.
15. D. Rappoport and F. Furche, *J. Chem. Phys.*, 2010, **133**, 134105.
16. TURBOMOLE v 6.4, a development of University of Karlsruhe and Forschungszentrum Karlsruhe GmbH, 2011.